Antiparallel Side-by-Side Heterodimer for Sequence-Specific Recognition in the Minor Groove of DNA by a Distamycin/1-Methylimidazole-2-carboxamide-netropsin Pair

Milan Mrksich and Peter B. Dervan*

Contribution from the Arnold and Mabel Beckman Laboratories of Chemical Synthesis, California Institute of Technology, Pasadena, California 91125

Received December 4, 1992

Abstract: The two peptides distamycin A (D) and 1-methylimidazole-2-carboxamide-netropsin (2-ImN) simultaneously bind the five-base-pair sequence 5′-TGTTA-3′. Footprinting experiments indicate that both molecules are necessary for binding to this sequence while affinity cleaving data define the orientations with which each peptide binds to this sequence. The footprinting and affinity cleaving data are consistent with a model wherein the two peptides bind as a side-by-side antiparallel heterodimer in the minor groove of double-helical DNA.

1:1 Peptide–DNA Complexes. The natural products netropsin and distamycin A (D) are crescent-shaped di- and tripeptides, respectively, that bind in the minor groove of DNA at sites of four or five successive A, T base pairs (bp).[1-3] The structures of a number of peptide–DNA complexes have been determined by X-ray diffraction[4] and NMR spectroscopy,[5] and the thermodynamic profiles have been studied for these complexes.[6] Analyses of these 1:1 peptide–DNA complexes have led to the conclusion that hydrogen bonding, van der Waals contacts, and electrostatics all contribute to the binding affinity and specificity. It has been found that the width of the minor groove of these A,T-rich sequences is narrower than that of standard B-DNA.[7] The two (or three) *N*-methylpyrrolecarboxamides twist in a screw sense to match the walls of the minor groove, giving a favorable shape complementarity for the ligand, while the carboxamide NH's participate in bifurcated hydrogen bonds to adenine N3 and thymidine O2 atoms on the floor of the minor groove (Figure 1).

Peptides Designed for Binding Mixed Sequences. Early efforts in designing peptides for the recognition of G,C base pairs were based on 1:1 peptide–DNA complexes and involved incorporating hydrogen bond acceptor atoms on ligands which could form
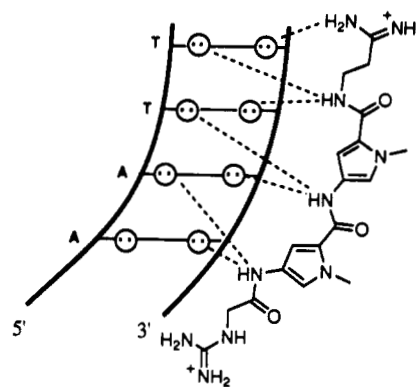

Figure 1. 1:1 Complex of netropsin with 5′-AATT-3′.[4a] Circles with dots represent lone pairs of N3 of purines and O2 of pyrimidines. Putative hydrogen bonds are illustrated by dashed lines.

specific hydrogen bonds to amino groups of guanine on the floor of the minor groove.[8-10] Distamycin analogs which substitute heteroatoms for the pyrrole C3 (e.g. imidazole and thiazole) display increased tolerance for G,C base pairs in their binding sites, but with an overall loss of specificity.[9] Remarkably, two synthetic peptides based on this 1:1 rationale display altered specificity for mixed sequences. Pyridine-2-carboxamide-netropsin (2-PyN) and 1-methylimidazole-2-carboxamide-netropsin (2-ImN) bind specifically to 5′-(A,T)G(A,T)C(A,T)-3′ sequences.[10,11] However, 1:1 models of 2-PyN·DNA and 2-ImN·DNA complexes seemed inadequate for rationalizing the recognition of G,C base pairs in both the second and fourth positions of the binding site.[10]

2:1 Peptide–DNA Complexes. Two-dimensional NMR studies by Wemmer and Pelton have revealed that distamycin at 2–4 mM concentrations is capable of binding in the minor groove of

(1) (a) Krylov, A. S.; Grokhovsky, S. L.; Zasedatelev, A. S.; Zhuze, A. L.; Gursky, G. V.; Gottikh, B. P. *Nucleic Acids Res.* **1979,** *6,* 289–304. (b) Zasedatelev, A. S.; Gursky, G. V.; Zimmer, Ch.; Thrum, H. *Mol. Biol. Rep.* **1974,** *1,* 337–342. (c) Zasedatelev, A. S.; Zhuze, A. L.; Zimmer, Ch.; Grokhovsky, S. L.; Tumanyan, V. G.; Gursky, G. V.; Gottikh, B. P. *Dokl. Akad. Nauk SSSR* **1976,** *231,* 1006–1009. (d) For a review, see: Zimmer, C.; Wähnert, U. *Prog. Biophys. Mol. Biol.* **1986,** *47,* 31–112.

(2) (a) Van Dyke, M. W.; Hertzberg, R. P.; Dervan, P. B. *Proc. Natl. Acad. Sci. U.S.A.* **1982,** *79,* 5470–5474. (b) Van Dyke, M. W.; Dervan, P. B. *Cold Spring Harbor Symp. Quant. Biol.* **1982,** *47,* 347–353. (c) Van Dyke, M. W.; Dervan, P. B. *Biochemistry* **1983,** *22,* 2373–2377. (d) Harshman, K. D.; Dervan, P. B. *Nucleic Acids Res.* **1985,** *13,* 4825–4835. (e) Fox, K. R.; Waring, M. J. *Nucleic Acids Res.* **1984,** *12,* 9271–9285. (f) Lane, M. J.; Dobrowiak, J. C.; Vournakis, J. *Proc. Natl. Acad. Sci. U.S.A.* **1983,** *80,* 3260–3264.

(3) (a) Schultz, P. G.; Taylor, J. S.; Dervan, P. B. *J. Am. Chem. Soc.* **1982,** *104,* 6861–6863. (b) Taylor, J. S.; Schultz, P. G.; Dervan, P. B. *Tetrahedron* **1984,** *40,* 457–465. (c) Schultz, P. G.; Dervan, P. B. *J. Biomol. Struct. Dyn.* **1984,** *1,* 1133–1147. (d) Dervan, P. B. *Science* **1986,** *232,* 464–471.

(4) (a) Kopka, M. L.; Yoon, C.; Goodsell, D.; Pjura, P.; Dickerson, R. E. *Proc. Natl. Acad. Sci. U.S.A.* **1985,** *82,* 1376–1380. (b) Kopka, M. L.; Yoon, C.; Goodsell, D.; Pjura, P.; Dickerson, R. E. *J. Mol. Biol.* **1985,** *183,* 553–563. (c) Coll, M.; Frederick, C. A.; Wang, A. H.-J.; Rich, A. *Proc. Natl. Acad. Sci. U.S.A.* **1987,** *84,* 8385–8389.

(5) (a) Patel, D. J.; Shapiro, L. *J. Biol. Chem.* **1986,** *261,* 1230–1240. (b) Klevitt, R. E.; Wemmer, D. E.; Reid, B. R. *Biochemistry* **1986,** *25,* 3296–3303. (c) Pelton, J. G.; Wemmer, D. E. *Biochemistry* **1988,** *27,* 8088–8096.

(6) (a) Markey, L. A.; Breslauer, K. *J. Proc. Natl. Acad. Sci. U.S.A.* **1987,** *84,* 4359–4363. (b) Breslauer, K. J.; Remeta, D. P.; Chou, W.-Y.; Ferrante, R.; Curry, J.; Zaunczkowski, D.; Synder, J. G.; Marky, L. A. *Proc. Natl. Acad. Sci. U.S.A.* **1987,** *84,* 8922–8926.

(7) Yoon, C.; Privé, G. G.; Goodsell, D. S.; Dickerson, R. E. *Proc. Natl. Acad. Sci. U.S.A.* **1988,** *85,* 6332–6336.

(8) For early examples of hybrid molecules for the recognition of mixed sequences, see: (a) Dervan, P. B.; Sluka, J. P. *New Synthetic Methodology and Functionally Interesting Compounds;* Elsevier: New York, 1986; pp 307–322. (b) Griffin, J. H.; Dervan, P. B. *J. Am. Chem. Soc.* **1987,** *109,* 6840–6842.

(9) (a) Lown, J. W.; Krowicki, K.; Bhat, U. G.; Skorobogaty, A.; Ward, B.; Dabrowiak, J. C. *Biochemistry* **1986,** *25,* 7408–7416. (b) Kissinger, K.; Krowicki, K.; Dabrowiak, J. C.; Lown, J. W. *Biochemistry* **1987,** *26,* 5590–5595. (c) Lee, M.; Chang, D. K.; Hartley, J. A.; Pon, R. T.; Krowicki, K.; Lown, J. W. *Biochemistry* **1988,** *27,* 445–455.

(10) (a) Wade, W. S.; Dervan, P. B. *J. Am. Chem. Soc.* **1987,** *109,* 1574–1575. (b) Wade, W. S. Ph.D. Thesis, California Institute of Technology, 1989.

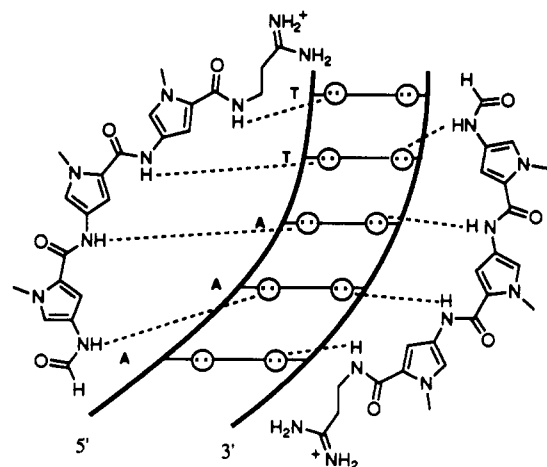(11) Wade, W. S.; Mrksich, M.; Dervan, P. B. *J. Am. Chem. Soc.* **1992,** *114,* 8783–8794.

Figure 2. 2:1 binding model for the complex formed between distamycin with a 5′-AAATT-3′ sequence.[12a] Circles with dots represent lone pairs of N3 of purines and O2 of pyrimidines. Putative hydrogen bonds are illustrated by dashed lines.

a 5′-AAATT-3′ sequence as a side-by-side antiparallel dimer (Figure 2).[12] An antiparallel dimer would explain the sequence specificity and orientation of (2-PyN)$_2$·5′-TGACT-3′ and (2-ImN)$_2$·5′-TGACT-3′ observed from footprinting and affinity cleaving data.[11] Indeed, the 2-ImN·5′-TGACT-3′ complex has now been characterized as a 2:1 complex directly by NMR spectroscopy (Figure 3).[13] The structure reveals that the two peptides bind in the minor groove as a side-by-side antiparallel dimer. In contrast to the distamycin homodimer, 2-ImN binds the 5′-TGACT-3′ sequence as a 2:1 complex at low ligand–DNA stoichiometries, indicating that the two peptides bind with positive cooperativity.[13] Simultaneously, Wemmer, Lown, and co-workers have characterized by NMR a distamycin analog containing a central imidazole in complex with a 5′-AAGTT-3′ sequence as a side-by-side antiparallel dimer.[14,15] These 2:1 models for peptide–DNA complexes differ in many respects from the well-characterized early 1:1 models observed for binding of distamycin and netropsin to A,T-rich DNA. The minor-groove width in the 2:1 complex is likely twice that observed in 1:1 models. With regard to specific hydrogen bonds in 1:1 complexes, distamycin and netropsin carboxamide NH's appear to form bifurcated hydrogen bonds to bases on *both strands of the DNA* (Figure 1). In the 2:1 motif, each ligand likely participates in hydrogen bonds only with bases on a *single strand* (Figures 2 and 3).

Design Rationale. Inspection of these 2:1 *homodimeric* models suggests that a *heterodimer* consisting of the two peptides D and 2-ImN may specifically bind to the family of sequences 5′-(A,T)G-(A,T)$_3$-3′. If one 2-ImN ligand in the (2-ImN)$_2$·5′-TGACT-3′ complex is replaced by a distamycin ligand, the absence of the imidazole N3 atom should favor an A,T base pair relative to a G,C base pair. In the proposed heterodimeric complex, the 2-ImN ligand forms a specific hydrogen bond to the guanine 2-amino group, followed by hydrogen bonds between the three carboxamide NH's with adenine N3 and thymine O2 atoms (Figure 4). The four carboxamide NH's of the distamycin ligand are expected to
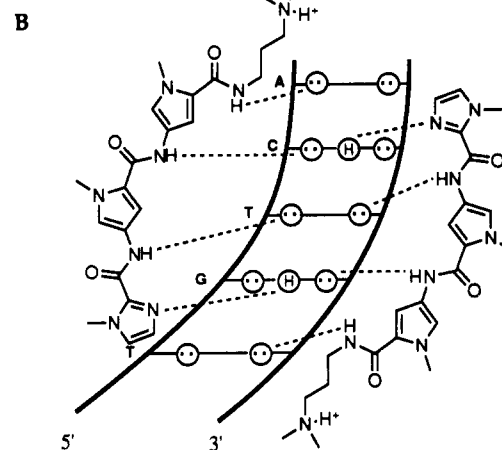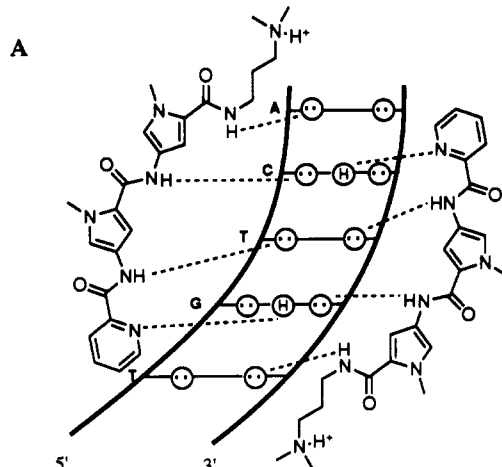

Figure 3. Homodimeric binding models for the complexes formed between (A) 2-PyN and (B) 2-ImN with the 5′-TGTCA-3′ sequence.[11] Circles with dots represent lone pairs of N3 of purines and O2 of pyrimidines. Circles containing an H represent the N2 hydrogen of guanine. Putative hydrogen bonds are illustrated by dashed lines.

Figure 4. Proposed heterodimeric binding model for the complex formed between D and 2-ImN with a 5′-(A,T)G(A,T)$_3$-3′ sequence. Circles with dots represent lone pairs of N3 of purines and O2 of pyrimidines. Circles containing an H represent the N2 hydrogen of guanine. Putative hydrogen bonds are illustrated by dashed lines.
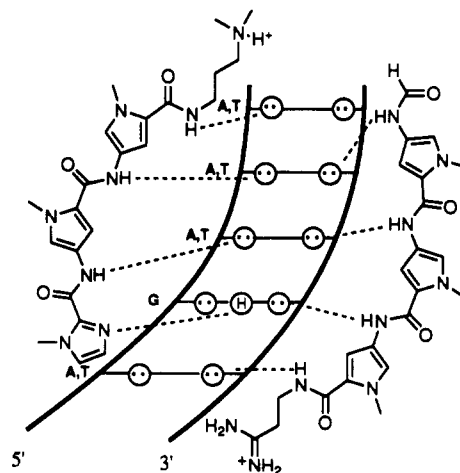
(12) (a) Pelton, J. G.; Wemmer, D. E. *Proc. Natl. Acad. Sci. U.S.A.* **1989**, *86*, 5723–5727. (b) Pelton, J. G.; Wemmer, D. E. *J. Am. Chem. Soc.* **1990**, *112*, 1393–1399.
(13) Mrksich, M.; Wade, W. S.; Dwyer, T. J.; Geierstanger, B. H.; Wemmer, D. E.; Dervan, P. B. *Proc. Natl. Acad. Sci. U.S.A.* **1992**, *89*, 7586–7590.
(14) Dwyer, T. J.; Geierstanger, B. H.; Bathini, Y.; Lown, J. W.; Wemmer, D. E. *J. Am. Chem. Soc.* **1992**, *114*, 5911–5919.
(15) The many recent reports of synthetic peptide analogs of distamycin and netropsin for the sequence-specific recognition of DNA will necessitate a consistent nomenclature for these molecules. We suggest that the peptides be named according to the sequence of heterocyclic residues, starting from the amino terminus. Netropsin and distamycin, consisting of two and three *N*-methylpyrrolecarboxamides, for example, could be designated P-P and P-P-P, respectively. Likewise, 2-ImN is designated Im-P-P, where Im = 1-methylimidazole-2-carboxamide. 2-ImD, the distamycin analog designed by Wemmer, Lown, and co-workers, would be designated P-Im-P.[14]

participate in hydrogen bonds with adenine N3, thymine O2, and cytosine O2 atoms. Overall, the *heterodimeric* complex can be thought of as a *hybrid* of the distamycin and 2-ImN *homodimeric* complexes.

Experimental Design. Footprinting and affinity cleaving experiments can be used to characterize this proposed complex. Neither D nor 2-ImN alone should protect a 5'-(A,T)G(A,T)₃-3' site from cleavage by the footprinting agent MPE·Fe(II).[2a-d] When both ligands are present, however, binding to this site by the heterodimer should protect the site from cleavage by MPE·Fe-(II). Affinity cleaving experiments would verify the requirement for both ligands in the complex and, in addition, define the *orientation* of each peptide in the proposed complex. Sequence-specific cleavage by 2-ImNE·Fe(II) on double-helical DNA should occur only in the presence of D. Furthermore, the cleavage pattern is expected to be proximal to the A,T-rich end of the 5'-(A,T)G-(A,T)₃-3' site, consistent with the orientation of 2-ImN which allows for a hydrogen bond to the guanine amino group (Figure 5A). Similarly, ED·Fe(II) is expected to effect sequence-specific cleavage only in the presence of 2-ImN. In a formal sense, D could bind in either a parallel or antiparallel orientation with respect to 2-ImN.[16] If the antiparallel heterodimer is favored, cleavage is expected to be near the 5' end of the 5'-TGTTA-3' strand of the binding site (Figure 5B). If the parallel heterodimer is favored, cleavage is expected to be near the 3' end of the 5'-TGTTA-3' binding site.

Results

Heterodimer Site Identification. Candidate heterodimer sites were identified by affinity cleavage experiments with ED·Fe(II) in the presence of varying concentrations of 2-ImN on radiolabeled restriction fragments from the plasmid pBR322 (as in Figure 5B). While a well-resolved site was not located, one strong site was found which overlapped a distamycin binding site. This region of cleavage corresponded to base pairs 90–100 on pBR322.[17] Two 34-base-pair oligonucleotides corresponding to this region, but with the overlapping distamycin site deleted, were prepared and used for footprinting and affinity cleaving experiments.[18]

Footprinting and Affinity Cleaving. Neither D at 2 μM nor 2-ImN at 100 μM alone protects any sites on the 34-base-pair oligonucleotide from cleavage by the footprinting agent MPE·Fe-(II) (pH 7.6 in 40 mM Tris–acetate and 20 mM NaCl at 22 °C) (Figure 6, lanes 4–6). The presence of both, D at 2 μM and 2-ImN at 100 μM, clearly protects the 5'-TGTTA-3' site from cleavage by MPE·Fe(II) (Figure 6, lane 7, Figure 7A). Affinity cleavage experiments verify the strict requirement for both ligands for binding to this site as well as define the orientation of each ligand in the complex. ED·Fe(II) at 5 μM affords no sequence-specific cleavage of the radiolabeled oligonucleotide (Figure 6, lane 8). In the presence of 100 μM 2-ImN, however, a cleavage pattern is observed exclusively at the 5' end of the 5'-TGTTA-3' strand of the binding site (Figure 6, lane 10, Figure 7B). Similarly, 2-ImNE·Fe(II) at 100 μM affords no sequence-specific cleavage but in the presence of 2 μM D reveals cleavage at the 3' end of the 5'-TGTTA-3' site (Figure 6, lanes 9 and 11, Figure 7C).

Concentration Dependence. The dependence of concentration of 2-ImN and D on cleavage by ED·Fe(II) and 2-ImNE·Fe(II), respectively, was investigated. ED·Fe(II) at 5 μM shows maximal cleavage in the presence of 2-ImN at 100 μM, which decreases with decreasing concentrations of 2-ImN. Higher concentrations of 2-ImN, however, also lead to a decrease in cleavage by ED·Fe-(II) (Figure 8, lanes 4–9). Similarly, 2-ImNE·Fe(II), at 100 μM, shows maximal cleavage in the presence of 2.5 μM D, decreasing with both higher and lower concentrations of D (Figure 8, lanes 10–15).

Discussion

Antiparallel Side-by-Side Heterodimer. The footprinting and affinity cleaving data are consistent with D and 2-ImN binding

(16) In the case of a heterodimeric complex, the term antiparallel refers to the amino to carboxy direction of the peptides in opposite alignment.

(17) (a) Sutcliffe, J. G. *Cold Spring Harbor Symp. Quant. Biol.* **1978**, *43*, 77–90. (b) Peden, K. W. C. *Gene* **1983**, *22*, 277–280.

(18) The 34-base-pair oligonucleotides corresponding to base pairs 77–110 of pBR322 have bases 90–91 changed from AA to GG to eliminate the 5'-AAATC-3' distamycin site.
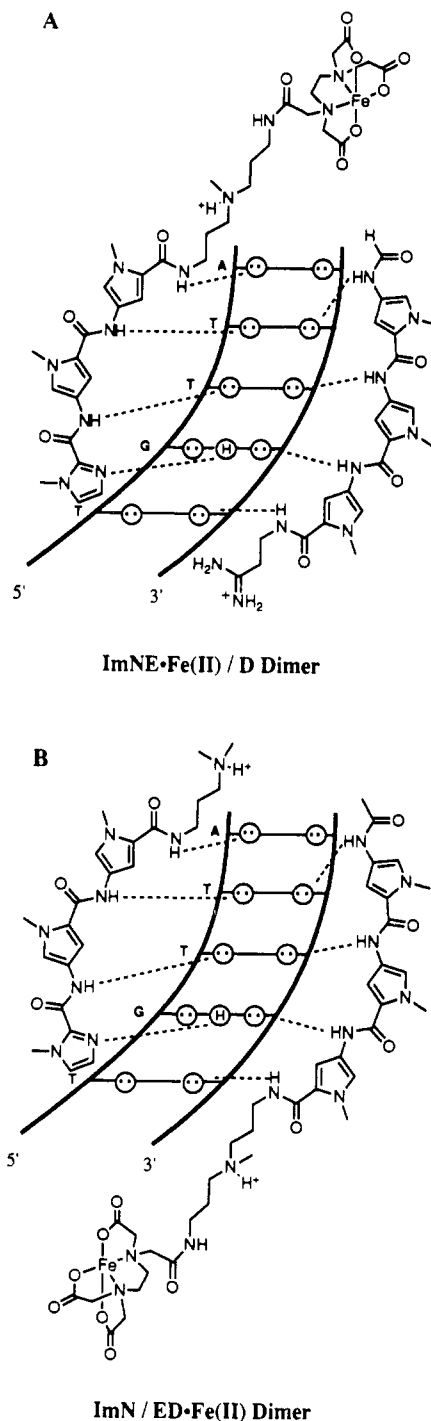
A

ImNE·Fe(II) / D Dimer

B

ImN / ED·Fe(II) Dimer

Figure 5. Experimental design for affinity cleaving experiments to determine the orientations of the peptides in the heterodimeric complex. 2:1 models for the heterodimeric complexes formed between (A) 2-ImNE·Fe(II) and D, and (B) ED·Fe(II) and 2-ImN, with the 5'-TGTTA-3' sequence. Circles with dots represent lone pairs of N3 of purines and O2 of pyrimidines. Circles containing an H represent the N2 hydrogen of guanine. Proposed hydrogen bonds are illustrated by dashed lines.

as an antiparallel side-by-side heterodimer in the minor groove of the 5'-TGTTA-3' sequence. The footprinting experiments clearly assign the binding site, and the affinity cleaving results unambiguously identify the orientation with which each peptide binds this site (Figure 9). Consistent with the proposed model, 2-ImN binds in the orientation which allows for a hydrogen bond between the imidazole N3 of 2-ImN and the guanine 2-amino group (Figure 4). While D can in principle bind with either orientation, the antiparallel arrangement is favored. This antiparallel orientation preference is not unexpected, as the parallel arrangement would place the two cationic ammonium groups in
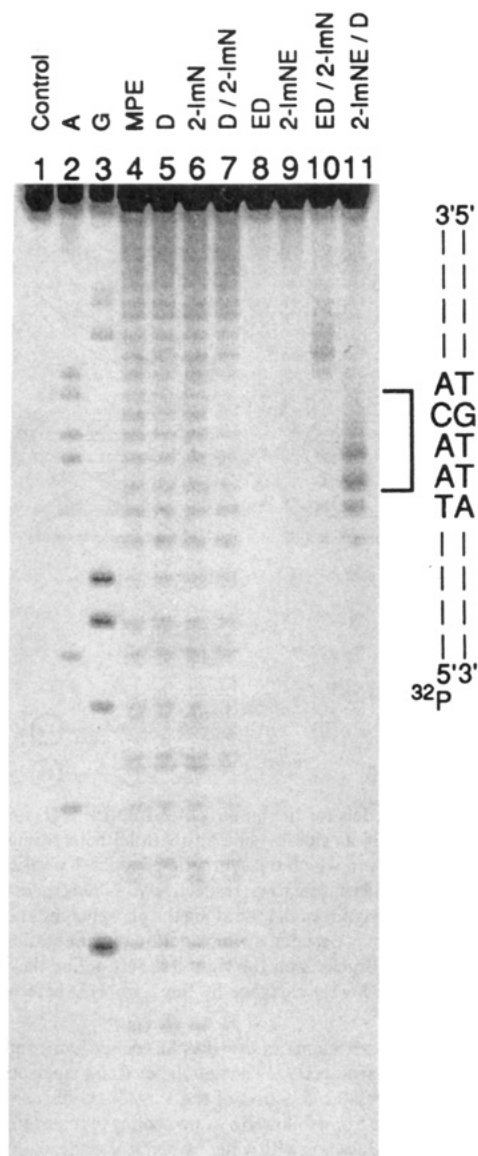
Figure 6. MPE·Fe(II) footprinting of D, 2-ImN, and D/2-ImN and affinity cleavage by ED·Fe(II), 2-ImNE·Fe(II), ED·Fe(II)/2-ImN, and 2-ImNE·Fe(II)/D. Gray-scale representation of a storage phosphor autoradiogram of a 20% denaturing polyacrylamide gel. There are 224 levels of gray representing a 50-fold change in the signal from the lowest (13 arbitrary units, white) to highest (600 arbitrary units, black) intensities. The 5′-TGTTA-3′ binding site is shown on the right side of the autoradiogram. All reactions contain 20 mM NaCl, 100 μM bp calf thymus DNA, and 20 kcpm 5′-labeled 34-base-pair oligonucleotide in 40 mM Tris–acetate pH 7.6 buffer. Lane 1, intact DNA; lane 2, A reaction; lane 3, G reaction; lane 4, MPE·Fe(II) standard; lane 5, 2 μM D; lane 6, 100 μM 2-ImN; lane 7, 2 μM D and 100 μM 2-ImN; lane 8, 5 μM ED·Fe(II); lane 9, 100 μM 2-ImNE·Fe(II); lane 10, 5 μM ED·Fe(II) and 100 μM 2-ImN; lane 11, 100 μM 2-ImNE·Fe(II) and 2 μM D. Lanes 4–7 contain 33 μM MPE·Fe(II).

proximity. Moreover, the energetic difference for the two alignments may reflect optimization of stacking interactions between the two peptides. We defer further speculation about this structure until NMR spectroscopic and thermodynamic data are available.

Sequence Specificity. An interesting observation in this heterodimeric complex is that D binds the 5′-TGTTA-3′ site with an apparent binding affinity nearly two orders of magnitude greater than does 2-ImN. This is also the approximate difference in binding affinities observed between D binding to A,T tracts of DNA and 2-ImN binding to 5′-(A,T)G(A,T)C(A,T)-3′ sequences. For the (2-ImN)$_2$·5′-TGACT-3′ complex, we suggested one reason for the overall lower free energy may be that the two guanine amino groups protruding from the floor of the
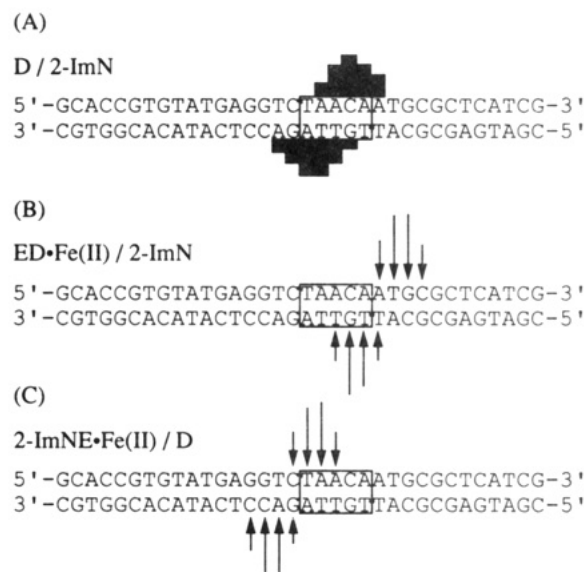

Figure 7. Histograms of cleavage protection (footprinting) and affinity cleavage data. (A) MPE·Fe(II) protection pattern for D and 2-ImN on the 34-base-pair oligonucleotide (Figure 6, lane 7). Bar heights are proportional to the protection from cleavage at each band. Boxes represent equilibrium binding sites determined by the published model.[2b] (B) Cleavage of the 34-base-pair oligonucleotide by ED·Fe(II) in the presence of 2-ImN (Figure 6, lane 10). (C) Cleavage of the 34-base-pair oligonucleotide by 2-ImNE·Fe(II) in the presence of D (Figure 6, lane 11). Arrows are proportional to the integrated densities of the cleavage bands. Boxes represent binding sites determined by the published model.[3b] Data for the top strands are shown in Figure 6.

minor groove do not allow the peptide ligands to sit as deeply in the minor groove.[11,13] In the heterodimeric complex, the imidazole N3 of 2-ImN is proposed to form a specific hydrogen bond to the guanine 2-amino group, which may also prohibit close contact between the peptide and the minor groove, consistent with the lower binding affinity. If D does not make specific contacts to the guanine 2-amino group, the peptide may be set deeper in the minor groove than 2-ImN, affording a more stable interaction.

For the 34-base-pair duplex studied here, the heterodimer consisting of D and 2-ImN shows a preference for cooperative 2:1 binding to the 5′-TGTTA-3′ site over 1:1 binding to other sites. However, we anticipate that, at higher concentrations of peptides, other binding sites available in large DNA can compete for the peptide ligands as either monomeric or homodimeric complexes (Figure 8). Perhaps, the specificity of the heterodimer could be further increased by covalently linking the two different peptides. An appropriate linker could disfavor monomeric or homodimeric binding by either D or 2-ImN as well as increase the affinity of the covalent heterodimer by diminishing the entropic penalty for complex formation.

Implications for the Design of Minor-Groove-Binding Molecules. While the 1:1 models based on the availability of high-resolution X-ray crystal structures of netropsin– and distamycin–DNA complexes[4] have proven to date inadequate for designing peptide analogs capable of binding mixed sequences with high specificities, the 2:1 models accurately predicted binding to a 5′-(A,T)G(A,T)$_3$-3′ sequence by the D/2-ImN heterodimer. This new design rationale differs significantly from earlier strategies in that each ligand is targeted to a single strand of the binding site in the minor groove of DNA, independent of the other ligand–strand interactions. However, it remains to be seen whether the 2:1 motif will serve as a general model for the design of peptide analogs which can bind other specific sequences in the minor groove of DNA.

Experimental Section

Materials. Distamycin A was purchased from Sigma. 2-ImN, 2-ImNE, and ED were synthesized and purified as previously described.[3b,11]
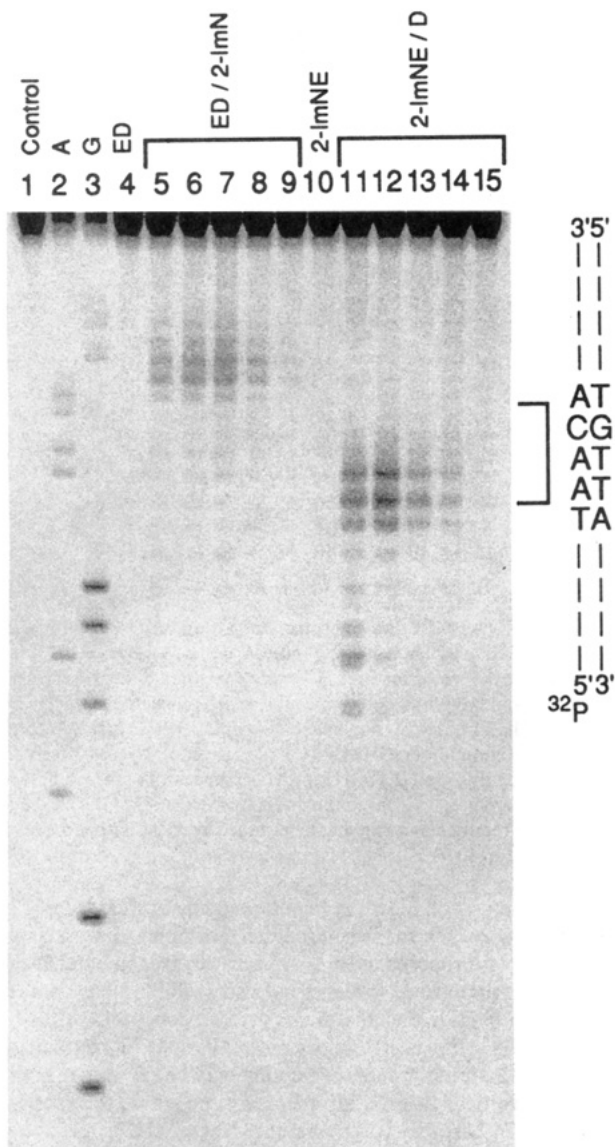
Figure 8. Concentration dependence of 2-ImN and D on specific cleavage by ED·Fe(II) and 2-ImNE·Fe(II), respectively. Gray-scale representation of a storage phosphor autoradiogram of a 20% denaturing polyacrylamide gel. There are 224 levels of gray representing a 50-fold change in the signal from the lowest (4 arbitrary units, white) to highest (200 arbitrary units, black) intensities. The 5'-TGTTA-3' binding site is shown on the right side of the autoradiogram. All reactions contain 10 mM DTT, 20 mM NaCl, 100 μM bp calf thymus DNA, and 20 kcpm 5'-labeled 34-base-pair oligonucleotide in 40 mM Tris–acetate pH 7.6 buffer. Lane 1, intact DNA; lane 2, A reaction; lane 3, G reaction; lanes 4–9 contain 5 μM ED·Fe(II); lane 5, 500 μM 2-ImN; lane 6, 200 μM 2-ImN, lane 7, 100 μM 2-ImN; lane 8, 50 μM 2-ImN; lane 9, 20 μM 2-ImN; lanes 10–15 contain 100 μM 2-ImNE·Fe(II); lane 11, 10 μM D; lane 12, 2.5 μM D; lane 13, 1.0 μM D; lane 14, 0.5 μM D; lane 15, 0.1 μM D.

Concentrations of the peptides were determined by UV spectroscopy using the following extinction coefficients: D (302 nm, ϵ = 35 000 cm^{-1} M^{-1}), ED (303 nm, ϵ = 35 000 cm^{-1} M^{-1}), 2-ImN (302 nm, ϵ = 26 000 cm^{-1} M^{-1}), and 2-ImNE (304 nm, ϵ = 26 500 cm^{-1} M^{-1}). Automated syntheses of oligonucleotides were performed on an ABI 380B DNA synthesizer using β-cyanoethyl phosphoramidite chemistry. The oligonucleotides were deprotected under standard conditions using ammonium hydroxide and purified by electrophoresis on 15% denaturing polyacrylamide gels. The gel bands were cut out, eluted, filtered through 0.45-μm Centres filters (Schleicher and Schuell), and precipitated with ethanol.[19] The concentrations of single-strand oligonucleotides were determined at 260 nm, using the following molar extinction coefficients for each base: 15 400 (A), 11 700 (G), 7300 (C), 8800 (T) cm^{-1} M^{-1}. The oligonucleotides were separately labeled at the 5' end with T4 polynucleotide
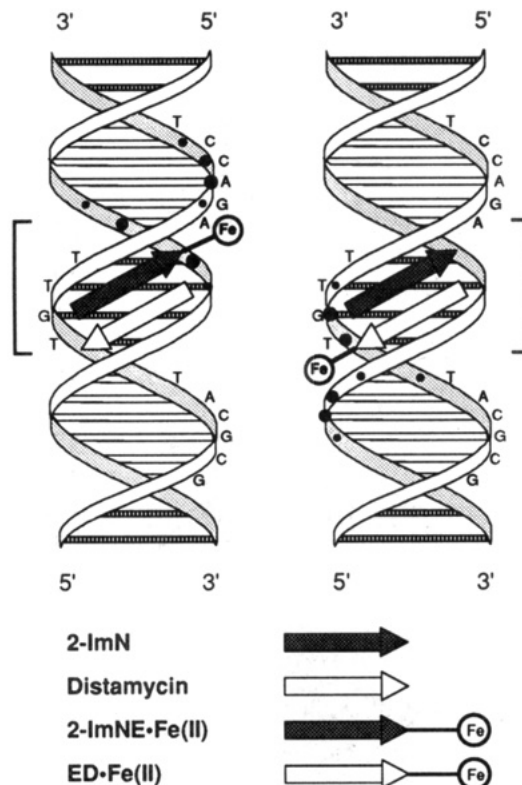

Figure 9. Ribbon models for the binding of 2-ImNE·Fe(II) and D, and ED·Fe(II) and 2-ImN as side-by-side antiparallel heterodimers in the minor groove of DNA in which the synthetic peptides 2-ImN and D are represented as gray and white arrows, respectively. Filled circles represent the intensities of cleavage at each base along the phosphodiester backbone from affinity cleavage experiments which define the orientation of each peptide (Figure 6). Brackets on the right and left define the sequence protected from MPE·Fe(II) cleavage by the 2-ImN/D heterodimer.

kinase (Boehringer-Mannheim) and γ-^{32}P ATP (Amersham) and purified by NICK column (Pharmacia).[19] The radiolabeled oligonucleotides were annealed with an excess (2–5 equiv) of the Watson–Crick complement by heating to 90 °C for 5 min followed by slow cooling to room temperature for 6 h and appropriate dilution with water. Chemical sequencing reactions were performed according to published methods.[20,21]

Footprinting and Affinity Cleavage Reactions. All reactions were executed in a total volume of 20 μL with final concentrations of each species as indicated. The ligands were added to solutions of radiolabeled oligonucleotide (20 000 cpm), calf thymus DNA (Pharmacia) (100 μM bp), Tris–acetate (40 mM, pH 7.6), and NaCl (20 mM) and incubated for 15 min at 22 °C. Footprinting reactions were initiated by the addition of MPE·Fe(II) (33 μM) and dithiothreitol (4 mM) and allowed to proceed for 15 min at 22 °C. Affinity cleavage reactions were initiated by the addition of dithiothreitol (10 mM) and allowed to proceed for 30 min at 22 °C. All reactions were stopped by precipitation with ethanol, resuspended in 100 mM Tris–borate–EDTA/80% formamide loading buffer, and electrophoresed on 20% polyacrylamide denaturing gels (5% cross-link, 7 M urea) at 1500 V for 6–8 h. The gels were analyzed using storage phosphor technology.

Quantitation by Storage Phosphor Technology Autoradiography. Photostimulable storage phosphor imaging plates (Kodak Storage Phosphor Screen S0230 obtained from Molecular Dynamics) were pressed flat against gel samples and exposed in the dark at 22 °C for 15–20 h. A Molecular Dynamics 400S PhosphorImager was used to obtain all data from the storage screens. The data were analyzed by performing volume integrations of all bands using the ImageQuant version 3.0 software running on an AST Premium 386/33 computer.

(19) Sambrook, J.; Fritsch, E. F.; Maniatis, T. *Molecular Cloning*; Cold Spring Harbor Laboratory: Cold Spring Harbor, NY, 1989.

(20) Iverson, B. L.; Dervan, P. B. *Nucleic Acids Res.* **1987**, *15*, 7823–7830.
(21) Maxam, A. M.; Gilbert, W. S. *Methods Enzymol.* **1980**, *65*, 499–560.